Status of tension between NOvA and T2K after Neutrino 2024 and possible role of nonstandard neutrino interactions

Sabya Sachi Chatterjee[1,*] and Antonio Palazzo[2,3,†]

[1]*Institut für Astroteilchenphysik, Karlsruher Institut für Technologie (KIT), Hermann-von-Helmholtz-Platz 1, 76344 Eggenstein-Leopoldshafen, Germany*

[2]*Dipartimento Interateneo di Fisica "Michelangelo Merlin", Via Amendola 173, 70126 Bari, Italy*

[3]*Istituto Nazionale di Fisica Nucleare, Sezione di Bari, Via Orabona 4, 70126 Bari, Italy*

(Received 29 September 2024; accepted 19 November 2024; published 3 December 2024)

In a previous work, we have shown that the data presented by the two long-baseline accelerator experiments NOvA and T2K at the Neutrino 2020 conference displayed a tension and that it could be alleviated by nonstandard neutrino interactions (NSI) of the flavor changing type involving the $e-\mu$ or the $e-\tau$ sectors with couplings $|\varepsilon_{e\mu}| \sim |\varepsilon_{e\tau}| \sim 0.1$. As a consequence, a hint in favor of NSI emerged. In the present paper, we reassess the issue in light of the new data released by the two experiments at the Neutrino 2024 conference. We find that the tension in the determination of the standard CP-phase $\delta_{\rm CP}$ extracted by the two experiments in the normal neutrino mass ordering persists and has a statistical significance of $\sim 2\sigma$. Concerning the NSI, we find that including their effects in the fit, the two values of $\delta_{\rm CP}$ preferred by NOvA and T2K return in very good agreement. The current statistical significance of the hint of nonzero NSI is $\sim 1.8\sigma$. Further experimental data are needed in order to settle the issue.

DOI: 10.1103/PhysRevD.110.113002

I. INTRODUCTION

The two long-baseline (LBL) accelerator experiments NOvA and T2K have recently released new data at the Neutrino 2024 Conference [1,2]. Interestingly, the results in the $\nu_\mu \to \nu_e$ appearance channel of the two experiments continue to be in tension confirming the trend observed in previous data released at the Neutrino 2020 Conference [3,4] (subsequently published in [5,6]) and point toward values of the CP-phase $\delta_{\rm CP}$ that are in disagreement when the data are interpreted in the standard three-flavor framework for normal ordered neutrino mass eigenstates.[1]

II. QUANTIFICATION OF TENSION

The mismatch between the preferred values of the $\delta_{\rm CP}$ is clear, with T2K preferring a value of $\delta_{\rm CP} \simeq 1.5\pi$ and NOvA indicating $\delta_{\rm CP} \simeq 0.9\pi$ (see Refs. [1,2]). Let's try to quantify the tension. Following [7], we introduce the function $\bar{\chi}^2(\delta_{\rm CP}) = \chi^2_{\rm T2K+NOvA}(\delta_{\rm CP}) - (\chi^2_{\rm T2K,min} + \chi^2_{\rm NOvA,min})$. Figure 1 shows the function $\bar{\chi}^2(\delta_{\rm CP})$ together with the two functions $\Delta\chi^2_r(\delta_{\rm CP}) = \chi^2_r(\delta_{\rm CP}) - \chi^2_{r,\rm min}$, where r is an index designating the experiment in question (T2K or NOvA). The level of compatibility between the two experiments can be quantified by means of the minimum value $\bar{\chi}^2_{\rm min} \simeq 6.3$, which for 2 d.o.f.[2] corresponds to a goodness of fit (GOF) of 4.3×10^{-2} (equivalent to 2.0σ).

An alternative method to quantify the tension is to compare the estimates of $\delta_{\rm CP}$ given by the two experiments. For T2K and NOvA, we assume that the errors are Gaussian. As suggested by Fig. 1, this assumption is reasonable for T2K, while for NOvA, it is valid only for the upper error, which is the relevant one for estimating the tension. We have for T2K $\delta_{\rm CP}/\pi = 1.47 \pm 0.24$, while for NOvA, $\delta_{\rm CP}/\pi = 0.87^{+0.20}_{-0.19}$. Considering the two errors summed in quadrature,

*Contact author: sabya.chatterjee@kit.edu
†Contact author: palazzo@ba.infn.it

[1]In the three-flavor framework, one introduces three mass eigenstates ν_i with masses m_i ($i = 1, 2, 3$), three mixing angles θ_{12}, θ_{13}, θ_{13}, and one CP-phase $\delta_{\rm CP}$. The neutrino mass ordering (NMO) is said to be normal (inverted) if $m_3 > m_{1,2}$ ($m_3 < m_{1,2}$). We will abbreviate normal (inverted) ordering as NO (IO).

[2]Note that the only two relevant d.o.f. are $\delta_{\rm CP}$ and θ_{23}. In fact, the parameters θ_{12}, Δm^2_{21} can be considered fixed by solar neutrinos and KamLAND, θ_{13} is fixed by Daya Bay, and Δm^2_{31} is fixed with high precision by the disappearance channel measurements of T2K and NOvA themselves. Concerning this last parameter, it is useful to notice that the estimate of Δm^2_{31} provided by the disappearance channel is completely insensitive to the couplings $\varepsilon_{e\mu}$ and $\varepsilon_{e\tau}$ within their range of interest, as we have explicitly checked numerically (see the right panels of Fig. S1 in the Supplemental Material [8]).

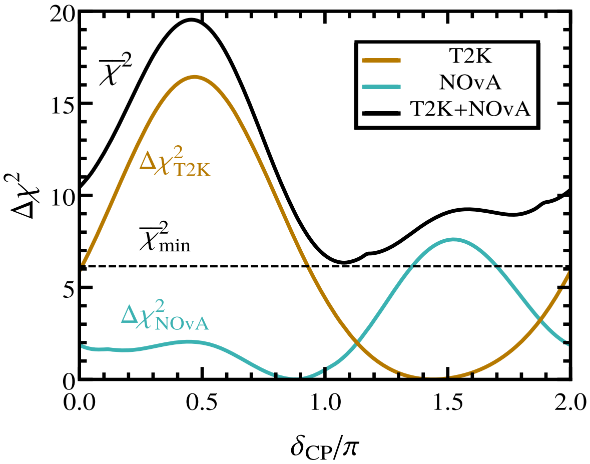

FIG. 1. Plot of the functions $\Delta\chi^2_{\rm T2K}$, $\Delta\chi^2_{\rm NOvA}$, and $\bar{\chi}^2$ as a function of $\delta_{\rm CP}$ for normal ordering.

we have that the two estimates differ by $\Delta\delta_{\rm CP}/\pi = 0.60 \pm 0.31$, hence corroborating the 2.0σ level of tension found with the first criterion.[3]

III. MOTIVATION FOR NSI

While the observed discrepancy may be induced by a statistical fluctuation or an unknown systematic error, it can represent a hint of new physics beyond the Standard Model (SM). As we already underlined in our previous paper [10], NOvA and T2K represent the ideal place to seek nonstandard matter effects in neutrino propagation due to their different and complementary setups. In particular, the two experiments work at two different peak energies (2 GeV for NOvA and 0.6 GeV for T2K) because of the different baselines (810 km for NOvA and 295 km for T2K). As a consequence, in NOvA matter effects are approximately three times larger with respect to T2K.

In [10] (see also [11]), we pointed out that the discrepancy could be solved by hypothesising the existence of NSI. More specifically, we found a $\sim 2\sigma$ level preference for nonzero complex neutral-current (NC) NSI of the flavor changing type involving the $e-\mu$ or the $e-\tau$ sectors with couplings $|\varepsilon_{e\mu}| \sim |\varepsilon_{e\tau}| \sim 0.1$.[4] In the present paper, we reassess the tension issue, showing that the indication persists in the new data with a statistical significance of 1.8σ.

[3]It is interesting to note that, as pointed out in [9], due to the cyclic nature of the $\delta_{\rm CP}$ parameter (which implies the violation of the hypotheses underlying the Wilk's theorem that become more apparent when the experiments have poor sensitivity to $\delta_{\rm CP}$), the real statistical level of the tension could be higher than that obtained using the χ^2 estimator or gaussian errors. An educated guess, based on the numerical simulations performed in [9] (see Fig. 1), is that a more faithful estimate of the statistical significance of the T2K-NOvA tension should lie somewhere in the interval $[2.0\sigma, 2.5\sigma]$.

[4]More precisely, the statistical significance of the indication we found in our previous paper [10] was at the 2.1σ level for $e-\mu$ NSI and 1.9σ level fro $e-\tau$ NSI.

IV. THEORETICAL FRAMEWORK

NSI may serve as the low-energy manifestation of high-energy physics, potentially arising from new, heavy states (for a review, see Refs. [12–16]). Alternatively, and perhaps more intriguingly, they could be linked to light mediators [17,18]. As first pointed out in [19], NSI can drastically modify the dynamics of neutrino flavor conversion while passing through matter [19–21]. The influence of NSI on current and upcoming long-baseline (LBL) neutrino experiments has been extensively studied (see, for example, [22–47]). In particular, the tension observed between the T2K and NOvA experiments has prompted numerous investigations into NSI [48–50] and other new physics scenarios, such as sterile neutrinos [51,52], nonunitary mixing [53,54], violations of Lorentz Invariance [55], vector leptoquarks [56], ultralight dark matter [57], Leggett-Garg inequality violations [58], and dark photons [59]. For a comprehensive review of these various scenarios, see Ref. [60].

The NSI of neutral current (NC) type can be expressed in terms of a dimension-six operator [19]:

$$\mathcal{L}_{\rm NC-NSI} = -2\sqrt{2}G_F\varepsilon^{fC}_{\alpha\beta}(\bar{\nu}_\alpha\gamma^\mu P_L\nu_\beta)(\bar{f}\gamma_\mu P_C f), \quad (1)$$

where $\alpha,\beta = e,\ \mu,\ \tau$ represent the neutrino flavors, and $f = e,\ u,\ d$ refer to the matter fermions. The projector operator P has a subscript $C = L,\ R$, which denotes the chirality of the fermion current, while $\varepsilon^{fC}_{\alpha\beta}$ are the NSI coupling amplitudes. The Hermiticity of the Hamiltonian imposes the condition:

$$\varepsilon^{fC}_{\beta\alpha} = (\varepsilon^{fC}_{\alpha\beta})^*. \quad (2)$$

For neutrinos propagating through the Earth, one can define the effective strength of the NSI couplings as

$$\varepsilon_{\alpha\beta} \equiv \sum_{f=e,u,d} \varepsilon^f_{\alpha\beta}\frac{N_f}{N_e} \equiv \sum_{f=e,u,d}(\varepsilon^{fL}_{\alpha\beta} + \varepsilon^{fR}_{\alpha\beta})\frac{N_f}{N_e}, \quad (3)$$

with N_f being the number density of f fermion. Since the Earth matter can be considered as neutral and isoscalar, with $N_n \simeq N_p = N_e$, we have $N_u \simeq N_d \simeq 3N_e$. Hence,

$$\varepsilon_{\alpha\beta} \simeq \varepsilon^e_{\alpha\beta} + 3\varepsilon^u_{\alpha\beta} + 3\varepsilon^d_{\alpha\beta}. \quad (4)$$

The NSI modify the effective Hamiltonian of neutrino in matter, which in the flavor basis can be expressed as

$$H = U\begin{bmatrix} 0 & 0 & 0 \\ 0 & k_{21} & 0 \\ 0 & 0 & k_{31} \end{bmatrix}U^\dagger + V_{\rm CC}\begin{bmatrix} 1+\varepsilon_{ee} & \varepsilon_{e\mu} & \varepsilon_{e\tau} \\ \varepsilon^*_{e\mu} & \varepsilon_{\mu\mu} & \varepsilon_{\mu\tau} \\ \varepsilon^*_{e\tau} & \varepsilon^*_{\mu\tau} & \varepsilon_{\tau\tau} \end{bmatrix}, \quad (5)$$

where U is the Pontecorvo-Maki-Nakagawa-Sakata (PMNS) matrix, which consists of three mixing angles $(\theta_{12}, \theta_{13}, \theta_{23})$ and the CP-phase $\delta_{\rm CP}$. We have denoted with

$k_{21} \equiv \Delta m^2_{21}/2E$ and $k_{31} \equiv \Delta m^2_{31}/2E$ the solar and atmospheric wave numbers respectively, with $\Delta m^2_{ij} \equiv m^2_i - m^2_j$, while $V_{\rm CC}$ represnts the charged-current matter potential

$$V_{\rm CC} = \sqrt{2} G_F N_e \simeq 7.6 Y_e \times 10^{-14} \left[\frac{\rho}{\rm g/cm^3}\right] \ {\rm eV}, \quad (6)$$

where $Y_e = N_e/(N_p + N_n) \simeq 0.5$ is the relative electron number density in the Earth crust. To facilitate the analysis of matter effects, it turns out to be useful to introduce the dimensionless parameter $v = V_{\rm CC}/k_{31}$, which gauges the sensitivity to matter effects. The magnitude of this parameter is given by

$$|v| = \left|\frac{V_{\rm CC}}{k_{31}}\right| \simeq 8.8 \times 10^{-2} \left[\frac{E}{\rm GeV}\right], \quad (7)$$

and it prominently features in the analytical form of the $\nu_\mu \to \nu_e$ conversion probability. Notably, in the two experiments, the first oscillation peak occurs at different energies with $E \simeq 0.6$ GeV for T2K and $E \simeq 2$ GeV for NOvA. Consequently, the matter effects in NOvA are approximately three times stronger ($v \simeq 0.18$) than in T2K ($v \simeq 0.05$). As previously discussed in [10], this heightened sensitivity makes NOvA particularly responsive to NSI, while T2K remains largely unaffected. This disparity may explain the apparent tension between the two experiments when interpreted within the standard three-flavor framework, ignoring NSI contributions.

In line with our earlier study [10], we focus on flavor nondiagonal NSI, where $\varepsilon_{\alpha\beta}$ for $\alpha \neq \beta$ plays a central role. Importantly, only these flavor changing NSI introduce dependence on a new CP-violating phase, which could be key to resolving the observed anomaly between NOvA and T2K. Specifically, we consider the parameters $\varepsilon_{e\mu}$ and $\varepsilon_{e\tau}$, which, as we will show below, induce an additional CP-phase dependence in the $\nu_\mu \to \nu_e$ transition probability.[5] Let us now consider the transition probability relevant for the T2K and NOvA experiments. When accounting for NSI, the probability can be expressed as the sum of three terms [65]:

$$P_{\mu e} \simeq P_0 + P_1 + P_2, \quad (8)$$

which, making use of a notation first introduced in [29], take the expressions

$$P_0 \simeq 4 s^2_{13} s^2_{23} f^2, \quad (9)$$

$$P_1 \simeq 8 s_{13} s_{12} c_{12} s_{23} c_{23} \alpha f g \cos(\Delta + \delta_{\rm CP}), \quad (10)$$

$$P_2 \simeq 8 s_{13} s_{23} v |\varepsilon| [a f^2 \cos(\delta_{\rm CP} + \phi) + b f g \cos(\Delta + \delta_{\rm CP} + \phi)], \quad (11)$$

$\Delta \equiv \Delta m^2_{31} L/4E$ being the atmospheric oscillating factor, L is the baseline and E the neutrino energy, and $\alpha \equiv \Delta m^2_{21}/\Delta m^2_{31}$. For compactness, we denote ($s_{ij} \equiv \sin\theta_{ij}$, $c_{ij} \equiv \cos\theta_{ij}$), and following [66], we introduce

$$f \equiv \frac{\sin[(1-v)\Delta]}{1-v}, \qquad g \equiv \frac{\sin v\Delta}{v}. \quad (12)$$

In Eq. (11), we have considered for the NSI coupling the complex form

$$\varepsilon_{\alpha\beta} = |\varepsilon_{\alpha\beta}| e^{i\phi_{\alpha\beta}}. \quad (13)$$

Notably, the form of P_2 is different for $\varepsilon_{e\mu}$ and $\varepsilon_{e\tau}$ and, in Eq. (11), one has to perform the substitutions

$$a = s^2_{23}, \qquad b = c^2_{23} \quad \text{if } \varepsilon = |\varepsilon_{e\mu}| e^{i\phi_{e\mu}}, \quad (14)$$

$$a = s_{23} c_{23}, \qquad b = -s_{23} c_{23} \quad \text{if } \varepsilon = |\varepsilon_{e\tau}| e^{i\phi_{e\tau}}. \quad (15)$$

In the expressions given in Eqs. (9)–(11), the sign of Δ, α and v is positive (negative) for NO (IO). The expressions of the probability given above are valid for neutrinos and the corresponding formulas for antineutrinos can be derived by inverting in Eqs. (9)–(11) the sign of all the CP-phases and of v. Finally, we notice that the third term P_2 depends on the (complex) NSI coupling and it is nonzero only in the presence of matter (i.e., if $v \neq 0$). Physically, it originates from the interference of the matter potential $\varepsilon_{e\mu} V_{\rm CC}$ (or $\varepsilon_{e\tau} V_{\rm CC}$) with the atmospheric wave number k_{31} (see Ref. [22]).

V. DATA USED IN THE ANALYSIS

We have made use of the datasets for the NOvA and T2K experiments from the most recent data releases, as presented in [1,2]. In our analysis, we have fully accounted for both the disappearance and appearance channels for each experiment. For the numerical simulations, we use the GLoBES software package [67,68] along with an additional public tool [69] designed to implement nonstandard interactions. To perform the analysis, we marginalized over θ_{13} using a 2.8% one sigma prior, with a central value of $\sin^2\theta_{13} = 0.0218$, as determined by the Daya Bay experiment [70]. The solar parameters Δm^2_{21} and θ_{12} are taken at their best fit values found in the global fit [71].

VI. NUMERICAL RESULTS

In Fig. 2, we present the numerical results obtained in the case of NO by combining NOvA and T2K. The three panels represent the projections in the planes spanned by each pair of the three parameters $|\varepsilon_{e\mu}|$, $\phi_{e\mu}$, and $\delta_{\rm CP}$. In all

[5] The $\nu_\mu \to \nu_\mu$ disappearance channel is sensitive to the $\mu - \tau$ NSI, but this can be safely ignored because of the very strong upper bound put with the atmospheric neutrinos by ANTARES [61], IceCube [62], and KM3NeT/ORCA6 [63], which all indicate $|\varepsilon_{\mu\tau}| \lesssim 5 \times 10^{-3}$ (see also [64] for a bound from Super-Kamiokande). Interestingly, all the three experiments find that $\varepsilon_{\mu\tau} = 0$ is disfavored slightly below the 90% C.L.

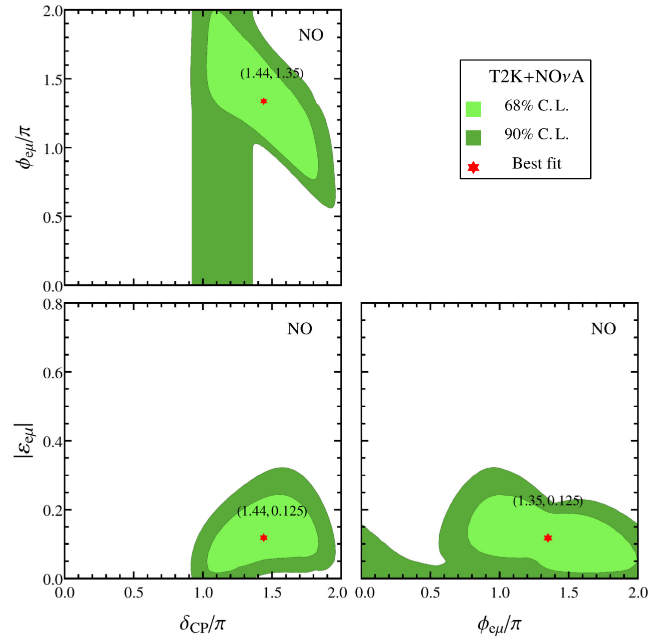

FIG. 2. Allowed regions determined by the combination of T2K and NOvA in NO for NSI of the $e-\mu$ type.

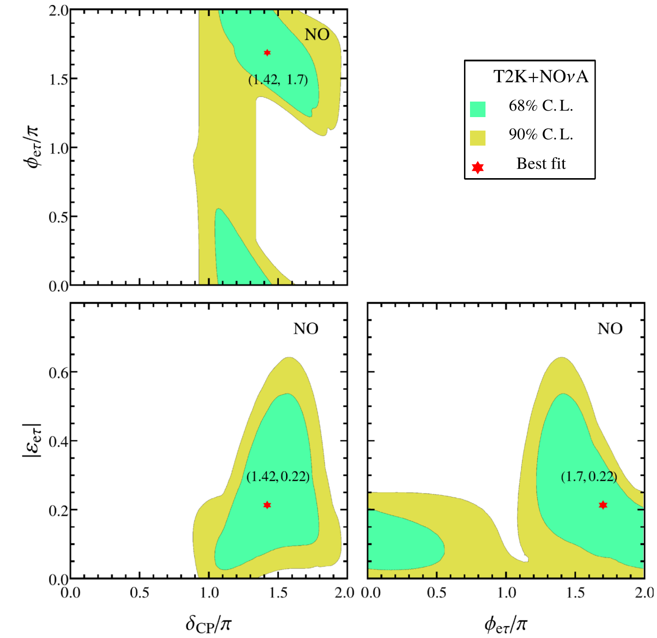

FIG. 3. Allowed regions determined by the combination of T2K and NOvA in NO for NSI of the $e-\tau$ type.

plots, the undisplayed parameters (θ_{23}, θ_{13}, and Δm^2_{31}) are marginalized. The regions displayed are those allowed at the 68% and 90% confidence level for 2 d.o.f. The first projection shows that both standard and nonstandard *CP*-phases have best fit values around 1.5π, with the standard *CP*-phase δ_{CP} being more constrained. The second and third panels represent the projections spanned by the NSI coupling and one of the two *CP*-phases. From these two plots, we observe that there is a preference for a NSI coupling different from zero with best fit $|\varepsilon_{e\mu}| = 0.125$ and statistical significance $\Delta\chi^2 = 3.1$ (corresponding to 1.76σ for 1 d.o.f.). Figure 3 is analogous to Fig. 2. In this case, however, the coupling considered is $\varepsilon_{e\tau}$ (with the associated *CP*-phase $\phi_{e\tau}$). The behavior of the *CP*-phases is similar to the previous case. The values preferred for the NSI coupling are larger with best fit $|\varepsilon_{e\tau}| = 0.22$. In this case, the statistical significance of the preference of nonzero NSI coupling is $\Delta\chi^2 = 3.2$ (corresponding to 1.79σ for 1 d.o.f.).

In Table I are reported the best fit values of the NSI couplings, those of the two *CP*-phases and what we obtain for $\Delta\chi^2 = \chi^2_{SM} - \chi^2_{SM+NSI}$ for each of the two possible choices of the neutrino mass orderings.[6] It is interesting to estimate at what statistical significance the SM hypothesis is rejected. For NO, in the case of $e-\mu$ and $e-\tau$ NSI, we obtain $\Delta\chi^2 = 3.1$ and $\Delta\chi^2 = 3.2$, respectively, which correspond (considering 2 d.o.f.) to an exclusion close to the 1.3σ level.

With the purpose of clarifying how the hint of a nonzero NSI coupling emerges, it is helpful to consider separately the two experiments NOvA and T2K. In Fig. 4, we show the allowed regions for the NO case, in the plane of the two parameters δ_{CP} and θ_{23}. The left panel depicts the SM scenario, while the central and right panels represent the SM + NSI cases with NSI of the $e-\mu$ and $e-\tau$ type, respectively. We underline that the SM regions in the left panel are in excellent agreement with those shown in the official plots of the collaborations [1,2], hence testifying the high level of accuracy reached by our analysis. In the central and right panels, the NSI parameters are fixed at the best fit obtained from the combination of NOvA and T2K. These correspond to $|\varepsilon_{e\mu}| = 0.125, \phi_{e\mu} = 1.35\pi$ (central panel) and $|\varepsilon_{e\tau}| = 0.22, \phi_{e\tau} = 1.70\pi$ (right panel). The two contours refer to the 68% and 90% C.L. for 2 d.o.f. In the SM case (left plot), a discrepancy between the values of δ_{CP} identified by the two experiments appears in a clear way, as already discussed above when commenting Fig. 1.

TABLE I. Best fit values and $\Delta\chi^2 = \chi^2_{SM} - \chi^2_{SM+NSI}$ for the two choices of the NMO.

NMO	NSI	$\lvert\varepsilon_{\alpha\beta}\rvert$	$\phi_{\alpha\beta}/\pi$	δ_{CP}/π	$\Delta\chi^2$
NO	$\varepsilon_{e\mu}$	0.13	1.35	1.44	3.1
	$\varepsilon_{e\tau}$	0.22	1.70	1.42	3.2
IO	$\varepsilon_{e\mu}$	0.05	1.44	1.52	0.94
	$\varepsilon_{e\tau}$	0.23	1.54	1.54	2.9

[6]Note that the best fit values we obtain for the complex NSI couplings $\varepsilon_{e\mu}$ and $\varepsilon_{e\tau}$ are almost pure imaginary (being $\phi_{e\mu}$ and $\phi_{e\tau}$ close to $\sim 1.5\pi$). For this reason, they cannot be confronted with the results of the NSI global analysis [72], where only real NSI couplings are considered. We may only observe qualitatively that the size $|\varepsilon_{e\mu}| = 0.125$ and $|\varepsilon_{e\tau}| = 0.22$ are compatible with the 90% C.L. reported in [72].

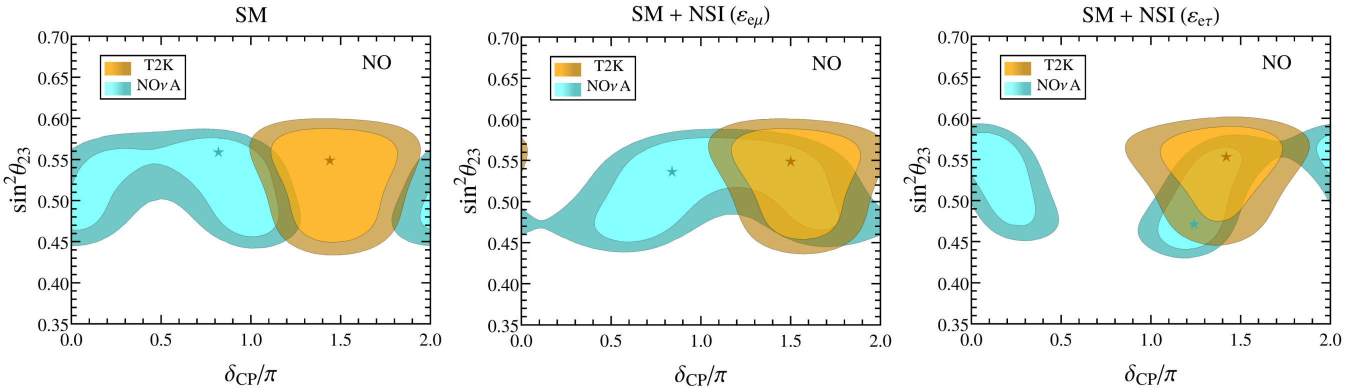

FIG. 4. Allowed regions by T2K and NOvA for NO in the SM case (left panel) and with NSI of the $e-\mu$ type (central panel) and of the $e-\tau$ type (right panel). In the central panel, we have taken the NSI parameters at their best fit values of the *combination* T2K + NOvA. These correspond to ($|\varepsilon_{e\mu}| = 0.125, \phi_{e\mu} = 1.35\pi$) for the central panel and ($|\varepsilon_{e\tau}| = 0.22, \phi_{e\tau} = 1.70\pi$) for the right panel. The contours correspond to the 68% and 90% C.L. for 2 d.o.f.

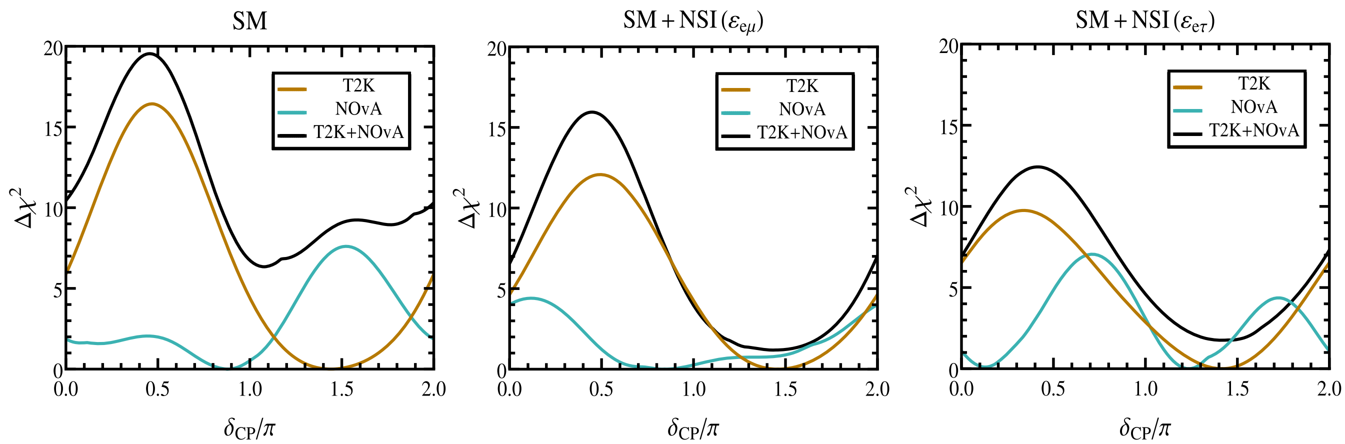

FIG. 5. Plot of the functions $\Delta\chi^2_{\rm T2K}$, $\Delta\chi^2_{\rm NOvA}$, and $\bar{\chi}^2$ as a function of $\delta_{\rm CP}$ for normal ordering. The left panel corresponds to the SM case (same as Fig. 1), and the other two panels represent the two NSI cases of $e-\mu$ type (central panel) and $e-\tau$ type (right panel). In the central panel, we have taken the NSI parameters at their best fit values of the *combination* T2K + NOvA as in Fig. 4.

The diminishment of the discrepancy among the two experiments attained when NSI are present is evident both in the central and right panels where there is a high level of overlap of the allowed regions for values of $\delta_{\rm CP}$ close to 1.5π. The different behavior between the central and the right panel is due to the different expression of transition probability for NSI of the $e-\mu$ or $e-\tau$ type. We can observe that the T2K regions are almost unaltered in the presence of NSI (due to low sensitivity of its setup to matter effects). Differently, the NOvA regions drastically change in the presence of NSI, due to the higher sensitivity to matter effects. These findings are in line with our analytical discussion and underline the high level of synergy and complementarity of the two setups.

In Fig. 5, we show the function $\bar{\chi}^2(\delta_{\rm CP})$ together with the two functions $\Delta\chi^2_r(\delta_{\rm CP}) = \chi^2_r(\delta_{\rm CP}) - \chi^2_{r,\rm min}$, where r is an index designating the experiment in question (T2K or NOvA). The left panel coincides with Fig. 1, which is reported here again for the sake of clearness, in order to facilitate the visual comparison with the cases corresponding to NSI presented in the central panel ($\varepsilon_{e\mu}$ case) and the right one ($\varepsilon_{e\tau}$ case). From these last two panels, it is clear how in the presence of NSI, the level of tension is substantially reduced, and it is basically negligible.[7]

[7]In this plot, we have decided to show the $\Delta\chi^2$ curves for T2K and NOvA for the best fit of their *combination* in order to facilitate the comparison of Fig. 5 with Fig. 4. Indeed, with this choice, the $\Delta\chi^2$ curves are exactly the 1D projections of the 2D regions of Fig. 4. Note, however, that for correctly estimating the GOF, one should consider (not shown) the curves corresponding to T2K and NOvA *marginalizing* over the NSI parameters ($\varepsilon_{e\mu}$ and $\phi_{e\mu}$ in the central panel and $\varepsilon_{e\tau}$ and $\phi_{e\tau}$ in the right panel). Clearly, in this case, there are 4 d.o.f (two oscillation parameters and two NSI parameters). Following this procedure, we find $\bar{\chi}^2_{\rm min} = 4.1$ for the $e-\mu$ case and $\bar{\chi}^2_{\rm min} = 4.5$ for $e-\tau$ case. Considering 4 d.o.f., these values correspond to a GoF $= 3.9 \times 10^{-1}$ and GoF $= 3.4 \times 10^{-1}$, respectively, which are both very high.

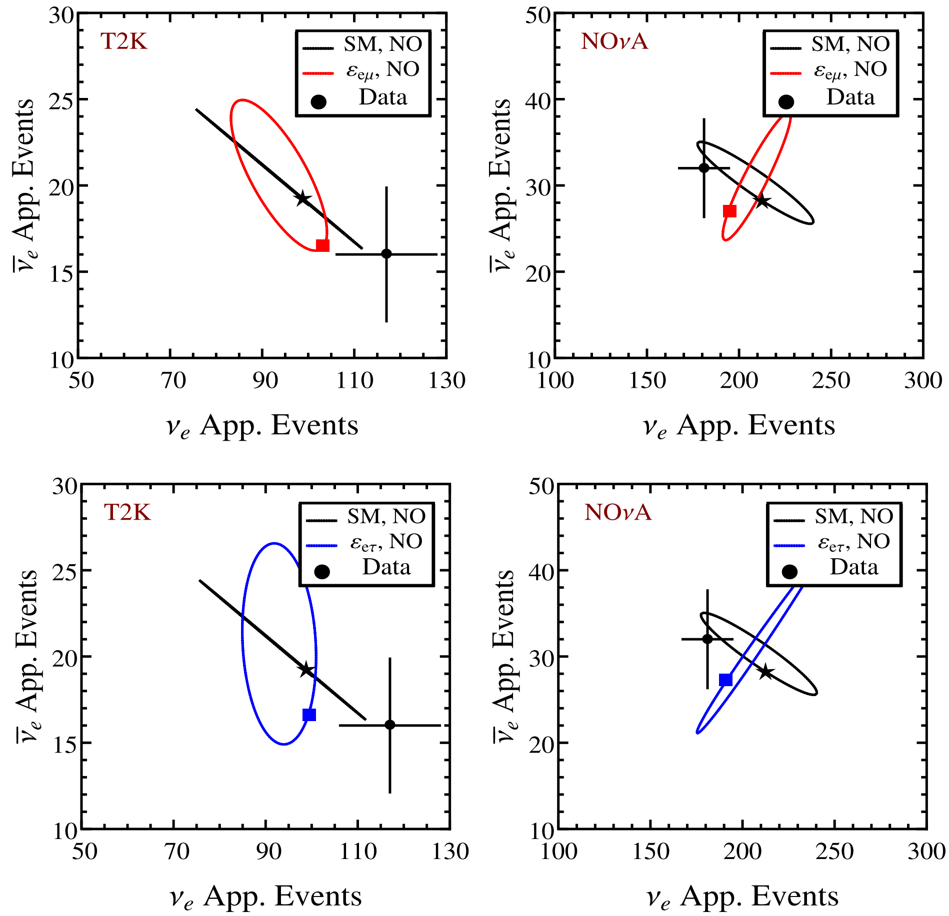

FIG. 6. Bievents plots for the T2K (left panels) and NOvA setup (right panels) for the NO case. The upper (lower) panels represent the case of $\varepsilon_{e\mu}(\varepsilon_{e\tau})$. Along all the ellipses the running parameter is the standard *CP* phase δ_{CP} in the range $[0, 2\pi]$. The black ellipses correspond to the SM case with best fit represented by stars. The colored ellipses correspond to the SM + NSI case with best fit indicated by squares. The ellipses and the best fit points located on them are determined by fitting the *combination* of T2K and NOvA. The points with the error bars display the experimental data with their statistical uncertainties.

As a further tool to interpret the results of the analysis, in Fig. 6, we show the bievents plots, in which on the x axis (y axis) is reported the number of detected electron neutrino (antineutrino) events. Such a graph is a guide to understanding the source of the tension between NOvA and T2K in the SM scenario and its alleviation in the presence of NSI. The plot is particularly insightful because in NOvA and T2K, almost all the information given in the appearance channel data is condensed in the number of events collected. In fact, due to the low statistics, the information contained in the shape of the energy spectrum is still limited. The ellipses displayed in the figure are plotted using the best fit parameters of the *combination* of T2K and NOvA. The relevant parameters are θ_{23}, θ_{13}, and Δm^2_{31} for the SM case. For the SM + NSI framework, one has also $|\varepsilon_{\alpha\beta}|$ and $\phi_{\alpha\beta}$. Both in the SM and SM + NSI cases, the running parameter along the ellipses is the *CP* phase δ_{CP} in the range $[0, 2\pi]$. The black ellipses correspond to the SM scenario with the stars representing the best fit point $\delta_{CP}^{SM} = 1.08\pi$. Such a value of δ_{CP} is a compromise among T2K (which push toward $\delta_{CP} = 1.5\pi$) and NOvA (which tends to prefer values close to 0.9π). The colored ellipses correspond the SM + NSI scenario (the squares designate the best fit value $\delta_{CP}^{NSI} \simeq 1.4\pi$, which is approximately the same in both the $e-\mu$ and $e-\tau$ options). The upper (lower) panels represent to the $e-\mu$ ($e-\tau$) scenario. From the plots, it is well visible how in the presence of the NSI, the best fit point of the model gets closer to the experimental data, thus reducing the tension found in the SM case. For completeness, in the Supplemental Material [8], we provide the additional figures S1–S5.

VII. CONCLUSIONS

In this paper, we have reassessed the issue of the tension between the measurements performed in the appearance channel by T2K and NOvA. The discrepancy first emerged at the Neutrino 2020 conference persists in the latest data released at Neutrino 2024 conference. We find that the disagreement can be resolved by nonstandard interactions (NSI) of the flavor changing type involving the $e-\mu$ and

$e - \tau$ flavors. Further experimental information is needed in order to settle the issue. The next data expected to come from T2K and NOvA will be crucial in this respect. Also, complementary information may be extracted from ANTARES, IceCube and KM3NeT/ORCA experiments, which are sensitive to the relevant NSI couplings. Most probably, however, if the current indication in favor of NSI will persist, only the future new-generation experiments DUNE and Hyper-Kamiokande will be able to definitely (dis)confirm it.[8]

Our results indicate the presence of effective NSI couplings of the order of 10%. Considering Eq. (4), these may translate into couplings of a few per ent for the fundamental particles (u and d quarks and electrons). Still, these are quite large couplings from a theoretical standpoint. In fact, if NSI are induced by mediators heavier than the electroweak scale, one naturally finds that the charged leptons are sensitive to new physics, on which there are strong limits. One possible way to avoid this issue is to augment the complexity of the model by considering dimension-8 operators [74], invoking radiative neutrino mass models (see, for example, the recent studies [75–77]) or calling in to play vector leptoquarks [56]. A radically different and fascinating option is to consider NSI induced by light or ultralight mediators, which are gaining increasing attention (see, for example, [17,18]). In this case, the NSI effects, due to the low momentum transfer, will be hardly visible in processes other than neutrino oscillations. As a matter of fact, the coherent forward scattering of neutrinos with ambient particles, operative at zero momentum transfer and observable through the modification of the oscillation probabilities, would provide the only way to probe new physics beyond SM in the neutrino sector.

We hope that our study may trigger investigations both at the experimental level, deepening the understanding of systematic uncertainties, and on the theoretical side, seeking new models able to predict the preferred NSI couplings.

[8]Note that these experiments may provide information on NSI also by observing astrophysical signals like those expected to come from supernova neutrinos (see for example [73]).

ACKNOWLEDGMENTS

We thank Enrique Fernández-Martínez and Thomas Schwetz for useful discussions. The work of S. S. C. is funded by the Deutsche Forschungsgemeinschaft (DFG, German Research Foundation)—Project No. 510963981. A. P. acknowledges partial support by the research Grant No. 2022E2J4RK “PANTHEON: Perspectives in Astroparticle and Neutrino THEory with Old and New messengers” under the program PRIN 2022 funded by the Italian Ministero dell’Università e della Ricerca (MUR) and by the European Union—Next Generation EU as well as partial support by the research project *TAsP* funded by the Instituto Nazionale di Fisica Nucleare (INFN).

DATA AVAILABILITY

No data were created or analyzed in this study.

[1] J. Wolcott, New neutrino oscillations results from NOνA with 10 years of data, in Talk Presented at Neutrino 2024 (2024), https://indico.fnal.gov/event/43209/timetable/#20200622.detailed.

[2] C. Giganti, T2K experiments status and plan, in Talk presented at Neutrino 2024 (2024), https://agenda.infn.it/event/37867/contributions/233954/attachments/121809/177671/Neutrino2024_T2K_Claudio.pdf.

[3] A. Himmel, New oscillations results from NOνA Experiment, in Talk Presented at Neutrino 2020: Virtual Meeting (2020), https://indico.fnal.gov/event/43209/timetable/#20200622.detailed.

[4] P. Dunne, Latest neutrino oscillations from T2K, in Talk presented at Neutrino 2020: Virtual Meeting (2020), https://indico.fnal.gov/event/43209/timetable/#20200622.detailed.

[5] M. A. Acero *et al.* (NOvA Collaboration), Improved measurement of neutrino oscillation parameters by the NOvA experiment, Phys. Rev. D **106**, 032004 (2022).

[6] K. Abe *et al.* (T2K Collaboration), Measurements of neutrino oscillation parameters from the T2K experiment using 3.6×10^{21} protons on target, Eur. Phys. J. C **83**, 782 (2023).

[7] M. Maltoni and T. Schwetz, Testing the statistical compatibility of independent data sets, Phys. Rev. D **68**, 033020 (2003).

[8] See Supplemental Material at http://link.aps.org/supplemental/10.1103/PhysRevD.110.113002 for additional figures.

[9] M. Blennow, P. Coloma, and E. Fernandez-Martinez, Reassessing the sensitivity to leptonic *CP* violation, J. High Energy Phys. 03 (2015) 005.

[10] S. S. Chatterjee and A. Palazzo, Nonstandard neutrino interactions as a solution to the *NOνA* and T2K discrepancy, Phys. Rev. Lett. **126**, 051802 (2021).

[11] P. B. Denton, J. Gehrlein, and R. Pestes, *CP*-violating neutrino nonstandard interactions in long-baseline-accelerator data, Phys. Rev. Lett. **126**, 051801 (2021).

[12] Y. Farzan and M. Tortola, Neutrino oscillations and nonstandard interactions, Front. Phys. **6**, 10 (2018).

[13] C. Biggio, M. Blennow, and E. Fernandez-Martinez, General bounds on nonstandard neutrino interactions, J. High Energy Phys. 08 (2009) 090.

[14] T. Ohlsson, Status of nonstandard neutrino interactions, Rep. Prog. Phys. **76**, 044201 (2013).
[15] O. G. Miranda and H. Nunokawa, Non standard neutrino interactions: Current status and future prospects, New J. Phys. **17**, 095002 (2015).
[16] P. S. Bhupal Dev *et al.*, Neutrino nonstandard interactions: A status report, SciPost Phys. Proc. **2**, 001 (2019).
[17] Y. Farzan, A model for large nonstandard interactions of neutrinos leading to the LMA-dark solution, Phys. Lett. B **748**, 311 (2015).
[18] Y. Farzan and I. M. Shoemaker, Lepton flavor violating nonstandard interactions via light mediators, J. High Energy Phys. 07 (2016) 033.
[19] L. Wolfenstein, Neutrino oscillations in matter, Phys. Rev. D **17**, 2369 (1978).
[20] S. Mikheev and A. Y. Smirnov, Resonance amplification of oscillations in matter and spectroscopy of solar neutrinos, Sov. J. Nucl. Phys. **42**, 913 (1985).
[21] S. Mikheev and A. Y. Smirnov, Resonant amplification of neutrino oscillations in matter and solar neutrino spectroscopy, Nuovo Cimento Soc. Ital. Fis. **9C**, 17 (1986).
[22] A. Friedland and I. M. Shoemaker, Searching for novel neutrino interactions at NOvA and beyond in light of large θ_{13}, arXiv:1207.6642.
[23] J. A. B. Coelho, T. Kafka, W. A. Mann, J. Schneps, and O. Altinok, Constraints for nonstandard interaction $\epsilon_{e\tau} V_e$ from ν_e appearance in MINOS and T2K, Phys. Rev. D **86**, 113015 (2012).
[24] I. Girardi, D. Meloni, and S. T. Petcov, The Daya Bay and T2K results on $\sin^2 2\theta_{13}$ and nonstandard neutrino interactions, Nucl. Phys. B **886**, 31 (2014).
[25] Z. Rahman, A. Dasgupta, and R. Adhikari, The discovery reach of *CP* violation in neutrino oscillation with nonstandard interaction effects, J. Phys. G **42**, 065001 (2015).
[26] P. Coloma, nonstandard interactions in propagation at the deep underground neutrino experiment, J. High Energy Phys. 03 (2016) 016.
[27] A. de Gouvêa and K. J. Kelly, nonstandard neutrino interactions at DUNE, Nucl. Phys. B **908**, 318 (2016).
[28] S. K. Agarwalla, S. S. Chatterjee, and A. Palazzo, Degeneracy between θ_{23} octant and neutrino nonstandard interactions at DUNE, Phys. Lett. B **762**, 64 (2016).
[29] J. Liao, D. Marfatia, and K. Whisnant, Degeneracies in long-baseline neutrino experiments from nonstandard interactions, Phys. Rev. D **93**, 093016 (2016).
[30] D. V. Forero and P. Huber, Hints for leptonic *CP* violation or new physics?, Phys. Rev. Lett. **117**, 031801 (2016).
[31] K. Huitu, T. J. Kärkkäinen, J. Maalampi, and S. Vihonen, Constraining the nonstandard interaction parameters in long baseline neutrino experiments, Phys. Rev. D **93**, 053016 (2016).
[32] P. Bakhti and Y. Farzan, *CP*-violation and nonstandard interactions at the moment, J. High Energy Phys. 07 (2016) 109.
[33] M. Masud and P. Mehta, Nonstandard interactions spoiling the *CP* violation sensitivity at DUNE and other long baseline experiments, Phys. Rev. D **94**, 013014 (2016).
[34] S. C and R. Mohanta, Implications of lepton flavor violation on long baseline neutrino oscillation experiments, Phys. Rev. D **94**, 053008 (2016).
[35] M. Masud and P. Mehta, nonstandard interactions and the resolution of ordering of neutrino masses at DUNE and other long baseline experiments, Phys. Rev. D **94**, 053007 (2016).
[36] A. de Gouvêa and K. J. Kelly, False signals of *CP*-invariance violation at DUNE, arXiv:1605.09376.
[37] S. Fukasawa, M. Ghosh, and O. Yasuda, Sensitivity of the T2HKK experiment to nonstandard interactions, Phys. Rev. D **95**, 055005 (2017).
[38] J. Liao, D. Marfatia, and K. Whisnant, Nonstandard neutrino interactions at DUNE, T2HK and T2HKK, J. High Energy Phys. 01 (2017) 071.
[39] J. Liao, D. Marfatia, and K. Whisnant, Nonmaximal neutrino mixing at NOνA from nonstandard interactions, Phys. Lett. B **767**, 350 (2017).
[40] M. Blennow, S. Choubey, T. Ohlsson, D. Pramanik, and S. K. Raut, A combined study of source, detector and matter nonstandard neutrino interactions at DUNE, J. High Energy Phys. 08 (2016) 090.
[41] K. N. Deepthi, S. Goswami, and N. Nath, Challenges posed by nonstandard neutrino interactions in the determination of δ_{CP} at DUNE, Nucl. Phys. B **936**, 91 (2018).
[42] L. J. Flores, E. A. Garces, and O. G. Miranda, Exploring NSI degeneracies in long-baseline experiments, Phys. Rev. D **98**, 035030 (2018).
[43] J. M. Hyde, Biprobability approach to *CP* phase degeneracy from nonstandard neutrino interactions, Nucl. Phys. B **949**, 114804 (2019).
[44] M. Masud, S. Roy, and P. Mehta, Correlations and degeneracies among the NSI parameters with tunable beams at DUNE, Phys. Rev. D **99**, 115032 (2019).
[45] I. Esteban, M. Gonzalez-Garcia, and M. Maltoni, On the determination of leptonic *CP* violation and neutrino mass ordering in presence of nonstandard interactions: Present status, J. High Energy Phys. 06 (2019) 055.
[46] F. Capozzi, S. S. Chatterjee, and A. Palazzo, Neutrino mass ordering obscured by nonstandard interactions, Phys. Rev. Lett. **124**, 111801 (2020).
[47] S. S. Chatterjee, P. S. B. Dev, and P. A. N. Machado, Impact of improved energy resolution on DUNE sensitivity to neutrino nonstandard interactions, J. High Energy Phys. 08 (2021) 163.
[48] B. Brahma and A. Giri, Discernible NSI effects in long-baseline neutrino experiments, arXiv:2302.09592.
[49] A. Cherchiglia, P. Pasquini, O. L. G. Peres, F. F. Rodrigues, R. R. Rossi, and E. S. Souza, Alleviating the present tension between T2K and NOνA with neutrino new physics at source, arXiv:2310.18401.
[50] M. A. Acero *et al.* (NOvA Collaboration), Search for *CP*-violating neutrino nonstandard interactions with the NOvA experiment, Phys. Rev. Lett. **133**, 201802 (2024).
[51] S. S. Chatterjee and A. Palazzo, Interpretation of NOνA and T2K data in the presence of a light sterile neutrino, arXiv:2005.10338.
[52] A. de Gouvêa, G. Jusino Sánchez, and K. J. Kelly, Very light sterile neutrinos at NOvA and T2K, Phys. Rev. D **106**, 055025 (2022).
[53] L. S. Miranda, P. Pasquini, U. Rahaman, and S. Razzaque, Searching for non-unitary neutrino oscillations in the present T2K and NOνA data, Eur. Phys. J. C **81**, 444 (2021).

[54] D. V. Forero, C. Giunti, C. A. Ternes, and M. Tortola, Nonunitary neutrino mixing in short and long-baseline experiments, Phys. Rev. D **104**, 075030 (2021).

[55] U. Rahaman, Looking for Lorentz invariance violation (LIV) in the latest long baseline accelerator neutrino oscillation data, Eur. Phys. J. C **81**, 792 (2021).

[56] R. Majhi, D. K. Singha, K. N. Deepthi, and R. Mohanta, Vector leptoquark U_3 and CP violation at T2K, NOvA experiments, Eur. Phys. J. C **82**, 919 (2022).

[57] H.-X. Lin, J. Tang, and S. Vihonen, Ultralight dark matter in neutrino oscillations to accommodate T2K and NOνA tension, arXiv:2312.11704.

[58] L. Konwar, J. Vardani, and B. Yadav, Violation of LGtI inequalities in the light of NOνA and T2K anomaly, Eur. Phys. J. C **84**, 1103 (2024).

[59] G. Alonso-Álvarez, J. M. Cline, B. Laurent, and U. Rahaman, Dark photon distortions of NOνA and T2K neutrino oscillations, arXiv:2407.13817.

[60] U. Rahaman, S. Razzaque, and S. U. Sankar, A review of the tension between the T2K and NOνA appearance data and hints to new physics, Universe **8**, 109 (2022).

[61] A. Albert *et al.* (ANTARES Collaboration), Search for nonstandard neutrino interactions with 10 years of ANTARES data, J. High Energy Phys. 07 (2022) 048.

[62] R. Abbasi *et al.* (IceCube Collaboration), Strong constraints on neutrino nonstandard interactions from TeV-Scale ν_u disappearance at IceCube, Phys. Rev. Lett. **129**, 011804 (2022).

[63] A. Lazo (KM3NeT Collaboration), Updated results on neutrino nonstandard interactions with KM3NeT/ORCA6, Proc. Sci., ICRC2023 (**2023**) 998.

[64] M. G. Aartsen *et al.* (IceCube Collaboration), Search for nonstandard neutrino interactions with IceCube DeepCore, Phys. Rev. D **97**, 072009 (2018).

[65] T. Kikuchi, H. Minakata, and S. Uchinami, Perturbation theory of neutrino oscillation with nonstandard neutrino interactions, J. High Energy Phys. 03 (2009) 114.

[66] V. Barger, D. Marfatia, and K. Whisnant, Breaking eight fold degeneracies in neutrino CP violation, mixing, and mass hierarchy, Phys. Rev. D **65**, 073023 (2002).

[67] P. Huber, M. Lindner, and W. Winter, Simulation of long-baseline neutrino oscillation experiments with GLoBES (General Long Baseline Experiment Simulator), Comput. Phys. Commun. **167**, 195 (2005).

[68] P. Huber, J. Kopp, M. Lindner, M. Rolinec, and W. Winter, New features in the simulation of neutrino oscillation experiments with GLoBES 3.0: General long baseline experiment simulator, Comput. Phys. Commun. **177**, 432 (2007).

[69] J. Kopp Sterile neutrinos and nonstandard neutrino interactions in GLoBES, https://www.mpi-hd.mpg.de/personalhomes/globes/tools/snu-1.0.pdf (2019).

[70] F. P. An *et al.* (Daya Bay Collaboration), Precision measurement of reactor antineutrino oscillation at kilometer-scale baselines by Daya Bay, Phys. Rev. Lett. **130**, 161802 (2023).

[71] F. Capozzi, E. Di Valentino, E. Lisi, A. Marrone, A. Melchiorri, and A. Palazzo, Unfinished fabric of the three neutrino paradigm, Phys. Rev. D **104**, 083031 (2021).

[72] P. Coloma, M. C. Gonzalez-Garcia, M. Maltoni, J. P. Pinheiro, and S. Urrea, Global constraints on nonstandard neutrino interactions with quarks and electrons, J. High Energy Phys. 08 (2023) 032.

[73] S. Jana and Y. Porto, nonstandard interactions of supernova neutrinos and mass ordering ambiguity at DUNE, arXiv:2407.06251.

[74] M. B. Gavela, D. Hernandez, T. Ota, and W. Winter, Large gauge invariant nonstandard neutrino interactions, Phys. Rev. D **79**, 013007 (2009).

[75] K. Babu, P. B. Dev, S. Jana, and A. Thapa, nonstandard interactions in radiative neutrino mass models, J. High Energy Phys. 03 (2020) 006.

[76] D. V. Forero and W.-C. Huang, Sizable NSI from the $SU(2)_L$ scalar doublet-singlet mixing and the implications in DUNE, J. High Energy Phys. 03 (2017) 018.

[77] U. K. Dey, N. Nath, and S. Sadhukhan, nonstandard neutrino interactions in a modified ν2HDM, Phys. Rev. D **98**, 055004 (2018).